

Improving the Safety of 3D Object Detectors in Autonomous Driving using IoGT and Distance Measures

Hsuan-Cheng Liao^{†‡}, Chih-Hong Cheng[§], Hasan Esen[†], Alois Knoll[‡]

Abstract—State-of-the-art object detectors are commonly evaluated based on accuracy metrics such as mean Average Precision (mAP). In this paper, inspired by the fact that mAP is not a direct safety indicator, we propose a straightforward safety metric, especially for 3D object detectors in Autonomous Driving contexts, by combining the Intersection-over-Ground-Truth (IoGT) measure and a distance ratio. Subsequently, we formulate a safety-aware loss function by amending IoGT to commonly used accuracy-oriented loss functions. Our experiments using models from the MMDetection3D library, the nuScenes dataset, and an in-house simulation dataset demonstrate that the object detector trained with our loss function significantly reduces unsafe predictions while staying performant on accuracy and maintaining good stability in the learning process.

I. INTRODUCTION

Object detection has been extensively studied and deployed in many domain applications, such as production line automation and automatic checkouts. Specifically, it refers to the function of simultaneously classifying and localizing potentially many objects within a single-frame input. Autonomous driving (AD) is one of these domains, as an automated vehicle (AV) needs the capability to detect objects in its surroundings to avoid collisions and drive safely. Still, one significant difference between AD and other domains is the safety-criticality in nature: It might be acceptable to miss an apple on a counter, but it certainly is not to miss a close-by pedestrian in front of the driving path.

Despite recent encouraging stories in deploying AVs in urban environments, scaling the results to multiple cities and mass production still has many challenges regarding safety assurance. Our work's focus lies in the realm of model testing, as we observe that most studies around object detection base their findings on accuracy metrics such as mean Average Precision (mAP), which in turn uses the Intersection-over-Union (IoU) measure [1]. However, it is possible that these accuracy metrics do not reflect well the actual safety of the AV and surrounding objects. Fig. 1 illustrates the concern.

[†]Hsuan-Cheng Liao and Hasan Esen are with DENSO AUTOMOTIVE Deutschland GmbH, 85386 Eching, Germany. h.liao, h.esen@eu.denso.com

[§]Chih-Hong Cheng is with Fraunhofer IKS, 80686 Munich, Germany. chih-hong.cheng@iks.fraunhofer.de

[‡]Hsuan-Cheng Liao and Alois Knoll are with Department of Informatics, Technical University of Munich, 85748 Garching, Germany. knoll@in.tum.de

* This project has received funding from the European Union's Horizon 2020 research and innovation programme under grant agreement No 956123 - FOCETA.



Scene			
	Prediction Ground truth		
Accuracy	Bad	Good	Best
Safety	Safe	Unsafe	Safe

Fig. 1: Even in some cases where the prediction is rather accurate (e.g., *center*), chances are it does not cover the object completely, leaving part of the object body being considered by the motion planner as free space.

To resolve the concern, our work proposes a safety metric as a direct reflector of safety by examining certain spatial properties. First, we identify a requirement containing two principles that an object detector has to follow:

- The predictions have to fully cover the targeted objects from the perspective of the AV (otherwise leaving a risk of collision at the uncovered parts of the objects);
- The predicted distances shall not be farther than the ground-truth object distances (otherwise over-estimating the object distances and leaving also a risk of collision).

Intuitively, this requirement shall help reduce certain risks of collision at the objects' front (per the AV's perspective). Technically, we find using 2D perspective-view (PV) and bird's-eye-view (BEV) projections of the 3D objects allows for a necessary and sufficient condition in modeling the two principles, respectively. In addition, we derive a quantitative variant of the metric for evaluating safety at a finer scale, using the Intersection-over-Ground-Truth (IoGT) measure and a distance ratio between the predictions and the ground truths. Although our idea is illustrated with a forward-driving perspective, it can be applied to sensors and object detectors facing other directions, achieving full coverage around an AV.

Apart from proposing the novel metric, we also consider how it can benefit the model construction process. For this, we design a safety-aware loss function that combines both accuracy and safety aspects. The reason for still modeling accuracy in the safety-aware loss function is that a pure consideration of safety might lead to overly conservative results. For instance, the object detector can place predictions just in front of the AV, stopping it from going anywhere. Flexible, the safety-aware loss function can be tuned to favor either accuracy or safety and be integrated during full training or fine-tuning processes. Besides the direct benefit of explicit safety considerations, our proposals can reduce

handshakes between the object detector and the subsequent processing pipeline, such as buffer design in motion planners, which are commonly difficult due to these components being developed by separate companies in the mass production of commercial vehicles.

We conduct experiments with state-of-the-art object detectors from the MMDetection3D library on two datasets [2]. The results demonstrate that testing with the proposed safety metric, compared to the standard mAP, allows for identifying many unsafe situations in object detection. In addition, the integration of the safety-aware loss function in training and finetuning sessions leads to a significant reduction in unsafe predictions while maintaining similar levels of accuracy as well as the stability in the learning process. In summary, our contributions include:

- A fundamental safety requirement for 3D object detectors in AD and its necessary and sufficient specification;
- A quantitative safety metric using IoGT and a distance ratio for practical safety evaluation 3D object detectors;
- A lightweight safety-aware loss function for optimizing models towards safety by design; and
- Empirical studies validating our proposals.

The remainder of the paper is organized as follows: Section II highlights the related works, including generic metrics and losses for object detection and safety assurance methods in AD. Section III introduces more details of the object detection task. Then, Section IV articulates the safety requirement and formulates a specification based on it. Section V and Section VI further synthesize the safety metric and loss function for evaluation and optimization, respectively. Section VII presents the experimental setting and results, and finally, Section VIII gives the summary of our work and outlook for future directions.

II. RELATED WORK

This section presents the related works on generic metrics and loss functions for object detection as well as safety assurance studies in AD.

A. Object Detection Metrics and Loss Functions

We briefly describe generic metrics and loss functions to motivate our research in the following. For more details, we defer readers to a recent survey paper [1].

The most widely accepted evaluation metric for object detection is mean Average Precision (mAP), which focuses on the accuracy of the predictions. However, the calculation steps of mAP involve many parameters, including the estimated confidence levels of the predictions, a predefined IoU threshold, and the Precision-Recall curve interpolation method [1]. To illustrate, recent survey papers [3], [4] find over ten variants of the above process. We observe two issues in such circumstances. First, reported results in existing studies might not be as sound as they seem. Evaluation parameters could be tuned in favor of better numeric scores. Second, it is not straightforward to see the connection between these accuracy metrics and safety properties. Therefore, in this work, we propose a sound

and practical process for the safety evaluation of 3D object detectors, i.e., *if given a full safety score, an object detector is guaranteed to have performed safely according to our safety requirement.*

We now review loss functions, an indispensable ingredient to guide data-driven models towards better performance. Generally, a loss function for an object detector can be separated into a classification and a localization element. For classification, the community has shifted from conventional losses such as Cross-Entropy Loss to Focal Loss [5] and its variants to prioritize hard negatives (e.g., wrong foreground classes). For localization, there have been two major branches. The first branch uses norm-based losses (e.g., L_1 , Smooth- L_1 , or L_2 norm) to independently penalize errors of BB parameters, including center or corner coordinates and dimensions. Although such formulations help disentangle the complex localization subtask, another branch of studies has found them not necessarily reflective of the localization correctness [6], [7]. Hence, loss functions directly engaging the IoU measure or its variants have been developed to improve the performance, possibly at the expense of slower convergences. Recently, some have proposed hybrid solutions, showing fast and accurate convergences [8], [9]. Their formulations usually contain both IoU-based and norm-based terms. Inspired by their work, we also attempt to formulate safety losses that can optimize object detectors for higher safety scores.

B. Safety Assurance in AD

As AVs advance rapidly with modern algorithms such as NNs, safety assurance for these systems has gathered more research focus. An overview of recent studies can be found in [10].

To highlight a few, there are system-level studies evaluating AVs with safety indicators such as mean time/distance between crashes/disengagements [11]. While these measurements generally give a good overview of the performance of the AVs, they do not provide deep insights into the component performance. For this, there have been methods and tools such as probabilistic model checking or testing frameworks for NNs [12]. We introduce several works dedicated to safety in the following and defer interested readers in general verification and validation (e.g., coverage-driven testing) to the survey paper [13]. One significant difference between safety-oriented research and other testing works is that the concept of safety is often task-specific. For example, in [14], the authors inspect practical considerations such as label ambiguity and misclassification tolerances for assessing the safety of 2D semantic segmentation models. Likewise, there have been studies integrating safety notions such as response time (based on the Responsibility-Sensitive Safety model [15]) into object detection and tracking metrics [16]. Lastly, to compensate potential insufficiency of NN models, some works introduce post-processing steps to correct the outputs of the models [17]–[19]. The results showcase a data-driven method [17], [18] and an analytical formulation [19],

based on the IoU measure, for expanding 2D predicted BBs and ensuring full enclosure of ground truths.

Our work complements those above in two ways. First, while most works focus on the IoU measure, we find IoGT particularly relevant to the safety of object detectors in AD. We additionally consider the third dimension (i.e., distance) in our formulations. Second, different from evaluation metrics and post-processing, we compose a safety-aware loss function for training or finetuning the models.

III. FOUNDATION

As introduced, an object detection task involves classifying and localizing objects in a single-frame input. Regardless of the input type, a camera image or lidar point cloud, an object detector predicts a set of detected objects encoded by their attributes, such as object class labels and locations. We denote the predictions as $\mathbf{PD} = \{\mathbf{PD}^i = [\mathbf{PD}^i_{c^i}, \mathbf{PD}^i_{\ell^i}] | i \in \mathbb{N}_M\}^1$, where M is the number of detected objects, $\mathbf{PD}^i_{c^i} \in \mathbb{N}_C$ is the class label and $\mathbf{PD}^i_{\ell^i} \in \mathbb{R}^L$ contains the location, dimensions and orientation of the i -th object. A common practice in object detection is to abstract objects with upright 3D BBs placed horizontally on the ground, as shown in Fig. 2 [1]. It follows that $\ell := {}_{3D}\mathbf{B} = [x_c, y_c, z_c, h, w, l, r] \in \mathbb{R}^7$, where $[x_c, y_c, z_c] = \mathbf{c} \in \mathbb{R}^3$ denotes the center of the BB, $[h, w, l] \in \mathbb{R}^3$ the BB dimensions, and $r \in \mathbb{R}$ the rotational angle around the gravitational direction (omitting the superscripts for prediction PD and the object index i).

For evaluation, there shall be a corresponding set of ground truths usually provided by human annotators, denoted as $\mathbf{GT} = \{\mathbf{GT}^i = [\mathbf{GT}^i_{c^i}, \mathbf{GT}^i_{\ell^i}] | i \in \mathbb{N}_N\}$. M could be different from N due to functional insufficiencies of the object detector or arguably human annotation ambiguities [14]. Post-processing, such as non-maximum suppression (NMS) or bipartite matching, is then employed to help relate the two sets of predicted and ground-truth objects. In the following sections, we assume ground truths are perfect without noises such as sensor failures or labeling errors, and M is equal to N . We also assume the AV is modeled as a point at the origin $\mathbf{o} := (0, 0, 0) \in \mathbb{R}^3$. Finally, it is noted that although our work targets cubic and rectangular object models (i.e., BBs), the same safety consideration can be applied to other forms, such as elliptical or B-spline object models [20].

IV. THE SAFETY REQUIREMENT AND SPECIFICATION

We state our safety requirement and formalize it into a specification in this section.

A. The Safety Requirement

In Section II-A, we have seen several metrics for evaluating the accuracy of object detector outputs against ground truths. Our work, on the contrary, aims at constructing a metric that evaluates the safety of object detector outputs, particularly in the context of AD. To such end, we propose a fundamental safety requirement for the object detector:

Requirement 1: Given an input, the object detector shall localize the objects such that the predictions entirely cover

their corresponding ground truths from the AV's perspective and that the predictions are estimated not farther than the ground truths.

The idea is depicted in Fig. 2. If Requirement 1 is fulfilled, then the object detector is said to be safe. The rationale is that as long as the object detector does not overestimate the object distances and covers the ground truths with predictions entirely, the motion planner shall react at least as safely as if the objects are detected at the ground-truth distances². Notably, Requirement 1 only handles what we call safety. As one may observe, the object detector will be evaluated safe if it simply places all predictions just in front of the AV, but it is not functionally effective in this way. One would still rely on the aforementioned accuracy metrics for distinguishing such cases. That is to say, our proposal does not replace the accuracy metrics but complements them with a notion of safety (as defined in Requirement 1). Likewise, we do not require correct classification. From a safety perspective, we argue that the AV should avoid colliding with any class of objects, and no object should be weighted more importantly than others. Nevertheless, class weighting mechanisms that can reflect more granular decision-making [21] may still be integrated. For now, we focus on our safety requirement (i.e., Requirement 1) and formalize it in the following.

B. Formalizing the Requirement into a Specification

For formalizing Requirement 1, we propose to use PV and BEV abstractions of the 3D BBs as shown in Fig. 2. Indeed, if one can ensure the predicted 3D BBs contain the ground-truth 3D BBs, Requirement 1 will be satisfied. However, we argue that this is not necessary. This is because, at any time during driving, one only cares about the frontal sides of the obstacles but not the back sides for avoiding a collision³. A predicted 3D BB can be smaller than (and hence not containing) the actual ground-truth 3D BB but still covers it from the AV's perspective. Therefore, to precisely formalize Requirement 1, we consider projecting the 3D BBs onto the PV and BEV planes.

We first address the PV projection. Essentially, during PV projection, a 3D BB is linearly projected onto an image plane using a center of projection (e.g., the origin) and an axis-aligned 2D BB will be placed over the projection. This

²In an AD pipeline, there is usually an object tracker and trajectory predictor in between the object detector and the motion planner. Concerning the two functional components' safety will introduce certain advantages and challenges. For example, an object could be misdetected in one of several consecutive frames as long as the object tracker is still aware of its existence. On the other hand, the relative velocity between the AV and the object has to be considered. Even if the object is estimated at a shorter distance by the object detector at time t and $t+1$, an inaccurate motion model calculated by the object tracker and the trajectory predictor might lead to unsafe path planning and, thus, a collision at time $t+2$. Nonetheless, these concerns are out-of-scope in our work, and we focus on single-frame outputs from object detection.

³Some argue that when attempting to overtake a preceding vehicle, one cares about the (invisible) back sides of the vehicle. Yet, we consider this more of an efficiency concern than safety. We focus on safely detecting an object such that there is a minimal risk of collision at its front. That said, when performing an overtake, some originally invisible back sides turn to be visible frontal sides and hence become relevant in our analysis.

¹Let $M \in \mathbb{N}$, $\mathbb{N}_M := \{x | 1 \leq x \leq M, x \in \mathbb{N}\}$ in our work.

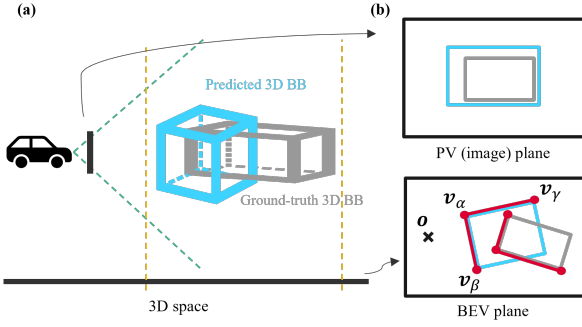


Fig. 2: 3D object abstractions via (a) 3D bounding boxes (BBs) and (b) 2D perspective-view (PV) and bird's-eye-view (BEV) BBs, which Requirement 1 and (2) employs. For simplicity, the actual object is not depicted but assumed to be contained in the ground-truth BB. The predictions are colored in blue and ground truths in grey. Additionally, on the BEV plane, the ego vehicle is marked by the black cross, and the BBs' close-to-AV vertices and frontal sides are highlighted in red.

results in a 2D PV BB defined as ${}_{PV}\mathbf{B} = [{}_{PV}x_c, {}_{PV}y_c, {}_{PV}h, {}_{PV}w] \in \mathbb{R}^4$, where $[{}_{PV}x_c, {}_{PV}y_c] \in \mathbb{R}^2$ denotes the center, and ${}_{PV}h \in \mathbb{R}$ and ${}_{PV}w \in \mathbb{R}$ the height and width. To ensure all predictions cover their ground truths, as stated in the first clause of Requirement 1, we define:

$${}_{PV}\Pi := \forall i \in \mathbb{N}_N : {}_{PV}^{GT}\mathbf{B}^i \subset {}_{PV}^{PD}\mathbf{B}^i, \quad (1)$$

where $\mathbf{P} \subset \mathbf{Q}$ denotes that BB \mathbf{P} is contained in BB \mathbf{Q} . In practice, this can be quickly checked with image coordinates of the 2D PV BB vertices.

Next, we project 3D BBs to 2D BEV BBs. This is done by outlining the smallest oriented 2D BB around the projected polygon of the 3D BB on the BEV plane (as shown in Fig. 3)⁴. Mathematically, this leads to ${}_{BEV}\mathbf{B} = [{}_{BEV}x_c, {}_{BEV}y_c, {}_{BEV}l, {}_{BEV}w, {}_{BEV}r] \in \mathbb{R}^5$, where $[{}_{BEV}x_c, {}_{BEV}y_c] \in \mathbb{R}^2$ is the center, ${}_{BEV}l \in \mathbb{R}$, ${}_{BEV}w \in \mathbb{R}$ and ${}_{BEV}r \in \mathbb{R}$ the length, width and the rotational angle around the gravitational direction. Now, based on (1), we consider adding two conditions for fully formalizing Requirement 1. First, the closest vertex of the predicted BEV BB has to be closer than the ground truth's. Second, the two frontal sides of the predicted BEV BB do not intersect with the ground-truth ones⁵. Altogether, we formalize Requirement 1 into a technical specification as:

$$\begin{aligned} \Pi = {}_{PV}\Pi \wedge \text{dist}_{BEV} \Pi \wedge \not\lrcorner \Pi \\ := \forall i \in \mathbb{N}_N : {}_{PV}^{GT}\mathbf{B}^i \subset {}_{PV}^{PD}\mathbf{B}^i \wedge \text{dist}({}_{BEV}^{PD}\mathbf{v}_\alpha^i) \leq \text{dist}({}_{BEV}^{GT}\mathbf{v}_\alpha^i) \\ \wedge \frac{{}_{BEV}^{PD}\mathbf{v}_\alpha^i \text{ } {}_{BEV}^{PD}\mathbf{v}_\beta^i}{{}_{BEV}^{GT}\mathbf{v}_\alpha^i \text{ } {}_{BEV}^{GT}\mathbf{v}_\beta^i} \not\lrcorner \frac{{}_{BEV}^{PD}\mathbf{v}_\alpha^i \text{ } {}_{BEV}^{PD}\mathbf{v}_\gamma^i}{{}_{BEV}^{GT}\mathbf{v}_\alpha^i \text{ } {}_{BEV}^{GT}\mathbf{v}_\gamma^i} \\ \wedge \frac{{}_{BEV}^{PD}\mathbf{v}_\alpha^i \text{ } {}_{BEV}^{PD}\mathbf{v}_\gamma^i}{{}_{BEV}^{GT}\mathbf{v}_\alpha^i \text{ } {}_{BEV}^{GT}\mathbf{v}_\gamma^i} \not\lrcorner \frac{{}_{BEV}^{PD}\mathbf{v}_\beta^i \text{ } {}_{BEV}^{PD}\mathbf{v}_\gamma^i}{{}_{BEV}^{GT}\mathbf{v}_\beta^i \text{ } {}_{BEV}^{GT}\mathbf{v}_\gamma^i}, \end{aligned} \quad (2)$$

⁴Even though we assumed upright 3D BBs in Sec. III, we depict the more extreme case of an oriented 3D BB in Fig. 3

⁵We note a special case where a BEV BB is perpendicularly facing the AV. In this case, our specification considers the front-facing side and either of the adjacent sides of the BEV BB

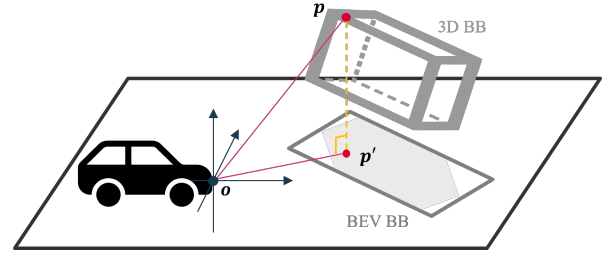


Fig. 3: Orthographic projection of a 3D ground-truth BB to a BEV 2D BB, where the 3D BB is possibly tilted due to undulating roads.

where $\overline{\mathbf{ab}} \not\lrcorner \overline{\mathbf{cd}}$ denotes that the two line segments do not intersect, and $\mathbf{v}_{\alpha/\beta/\gamma}$ are the close-to-AV vertices as highlighted in Fig. 2b.

As such, we ensure that the predictions cover the ground truths and are estimated not farther than them. We state two remarks at this point to further justify our usage of PV and BEV BBs. First, it is necessary to have the BEV conditions (i.e., $\text{dist}_{BEV} \Pi \wedge \not\lrcorner \Pi$) for satisfying Requirement 1. This is because the fact that a predicted 2D PV BB contains its ground-truth counterpart (i.e., ${}_{PV}\Pi$) does not imply that the 3D prediction is made in front of the 3D ground truth from the AV. A counterexample is as follows: The predicted 3D BB could be farther yet much larger than the ground-truth 3D BB such that after a perspective projection, the predicted 2D PV BB still covers its ground-truth counterpart. Therefore, one needs the 2D BEV conditions.

The second remark is that having the 2D PV condition (i.e., ${}_{PV}\Pi$) increases the precision of formalizing Requirement 1 into a specification. Similar to the case of 3D BB abstraction, 2D BEV BB abstraction can soundly satisfy Requirement 1 on its own. For instance, one can specify that predicted 2D BEV BBs shall fully contain ground-truth 2D BEV BBs⁶. However, this is also not necessary. With the 2D PV condition, one only has to specify the two additional 2D BEV conditions regarding the closest vertex and the frontal sides. Thus, our formalized Specification Π gives the necessary and sufficient conditions to Requirement 1.

V. A SAFETY METRIC FOR MODEL EVALUATION

We now leverage the analysis in the previous section and synthesize a safety metric for evaluating object detectors.

A. Qualitative Safety Metric

We first write the safety metric in a qualitative manner. To illustrate, it is responsible for evaluating whether a set of outputs of an object detector, when compared against the set of corresponding ground truths, is safe or not. With the specification in (2), we can formulate it as follows:

$$S_{q1}(\widetilde{PD}, \widetilde{GT}) := \Pi ? 1 : 0. \quad (3)$$

⁶The soundness of this BEV specification is attributed to the geometric property of orthographic projection. Specifically, as shown in Fig. 3, it always holds that $\overline{\mathbf{op}} \geq \overline{\mathbf{op}'}$. Additionally, the BEV BB always contains the projected polygon, hence the soundness.

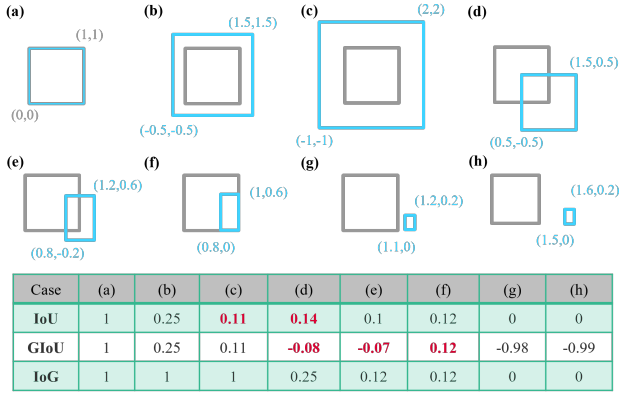


Fig. 4: A comparison of IoU, GIoU, and IoGT. The ground truth BB (in grey) is always spanning from (0,0) to (1,1), and the prediction (in blue) varies over cases. The values in red highlight the cases where the metric fails to model our safety notion.

B. Quantitative Safety Metric

We turn our focus on formulating a quantitative variant of the safety metric, which should take a similar responsibility to the qualitative one yet on a finer scale. More specifically, when the object detector performs safely (i.e., fulfilling Specification (2)), it is given a full score (e.g., at 1); when it does not, it is given a numeric value reflecting how unsafe the prediction is (e.g., from 1 to 0)⁷.

We first consider the 2D PV term in (2). Based on our safety specification, the more a predicted BB covers the ground-truth BB, the higher score it should generate. We notice, however, that the commonly used Intersection-over-Union (IoU) measure or its variants (e.g., Generalized-IoU (GIoU) [7]) do not reflect this property well. Instead, it is better modeled by Intersection-over-Ground-Truth (IoGT), defined in (4). Fig. 4 depicts different cases for comparing the measures. As a result, we utilize IoGT and define the PV-plane score as follows:

$$\begin{aligned}
 {}_{\text{PV}}S_{\text{qn}}(\widetilde{\mathbf{PD}}, \widetilde{\mathbf{GT}}) &:= \frac{1}{N} \sum_{i=1}^N \text{IoGT}(\mathbf{PD}_{\text{PV}}^i, \mathbf{GT}_{\text{PV}}^i) \\
 &= \frac{1}{N} \sum_{i=1}^N \frac{\text{area}(\mathbf{PD}_{\text{PV}}^i \cap \mathbf{GT}_{\text{PV}}^i)}{\text{area}(\mathbf{GT}_{\text{PV}}^i)}.
 \end{aligned} \quad (4)$$

Next, we consider the 2D BEV conditions. As shown in Fig. 5, the BEV-plane score should reflect the following cases differently: (a) If the closest vertex of the prediction $\mathbf{PD}_{\text{BEV}}^i$ is closer than that of the ground truth $\mathbf{GT}_{\text{BEV}}^i$ and the frontal sides don't intersect, then the particular prediction is said safe and given a full score (e.g., 1); (b) If $\mathbf{PD}_{\text{BEV}}^i$ is farther than $\mathbf{GT}_{\text{BEV}}^i$, then safety is quantified with the distance ratio and IoGT between the prediction and the ground truth; (c/d) If $\mathbf{PD}_{\text{BEV}}^i$ is closer than $\mathbf{GT}_{\text{BEV}}^i$ but the frontal sides intersect,

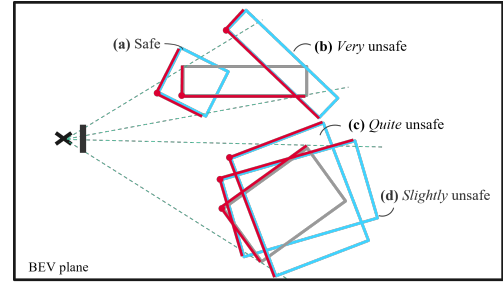


Fig. 5: Different cases of safety evaluation on the BEV plane (all fulfilling the PV-space specification, though). The predictions are in blue, the ground truths in grey, and the closest vertices and frontal sides in red.

then safety is quantified by the IoGT measure⁸. Now, we mathematically summarize the cases as follows:

$$\begin{aligned}
 {}_{\text{BEV}}S_{\text{qn}}(\widetilde{\mathbf{PD}}, \widetilde{\mathbf{GT}}) \\
 := \frac{1}{N} \sum_{i=1}^N \left[\min\left(1, \frac{\text{dist}(\mathbf{GT}_{\text{BEV}}^i \mathbf{v}_\alpha)}{\text{dist}(\mathbf{PD}_{\text{BEV}}^i \mathbf{v}_\alpha)}\right) \times \text{IoGT}(\mathbf{PD}_{\text{BEV}}^i, \mathbf{GT}_{\text{BEV}}^i) \right]
 \end{aligned} \quad (5)$$

To summarize, we combine the above PV and BEV terms into two versions of the quantitative safety metric. The first one is based on averaging as follows:

$$S_{\text{qn}}^{\text{sum}}(\widetilde{\mathbf{PD}}, \widetilde{\mathbf{GT}}) := \frac{1}{2} ({}_{\text{PV}}S_{\text{qn}} + {}_{\text{BEV}}S_{\text{qn}}). \quad (6)$$

The second one is based on multiplication as follows:

$$\begin{aligned}
 S_{\text{qn}}^{\text{pdt}}(\widetilde{\mathbf{PD}}, \widetilde{\mathbf{GT}}) &:= \frac{1}{N} \sum_{i=1}^N \left\{ \text{IoGT}(\mathbf{PD}_{\text{PV}}^i, \mathbf{GT}_{\text{PV}}^i) \right. \\
 &\quad \times \min\left(1, \frac{\text{dist}(\mathbf{GT}_{\text{BEV}}^i \mathbf{v}_\alpha)}{\text{dist}(\mathbf{PD}_{\text{BEV}}^i \mathbf{v}_\alpha)}\right) \times \text{IoGT}(\mathbf{PD}_{\text{BEV}}^i, \mathbf{GT}_{\text{BEV}}^i) \left. \right\}.
 \end{aligned} \quad (7)$$

VI. A SAFETY-AWARE LOSS FUNCTION FOR MODEL OPTIMIZATION

In this section, we further formulate a safety-aware loss function for optimizing 3D object detectors. As discussed in Section II-A, there have been multiple proposals in the literature aligning the optimization loss functions with the evaluation metrics, eventually generating stronger performances [6]–[9]. Likewise, we construct our loss function based on the quantitative safety metric, in which the IoGT measure plays a central role. Hence, we define a safety loss component $L_{\text{IoGT}} = 1 - \text{IoGT}(\mathbf{PD}_{\text{3D}}^i, \mathbf{GT}_{\text{3D}}^i)$, where $\text{IoGT}(\cdot, \cdot)$ now takes 3D BB inputs and computes the ratio using volumes of the BBs. This is due to the consideration that the task is performed directly in the 3D space and the availability of computing algorithms such as Pytorch3D [22]. Otherwise, 2D cases follow similarly.

As seen in Fig. 4, the safety loss component on its own does not suffice for optimizing an object detector as IoGT

⁷As discussed in Section IV-A, among safe predictions, there is no notion of “safer”. They are equally safe, though potentially unequally accurate.

⁸We note that during quantitative evaluation using the BEV conditions, we fall back to requiring ground-truth BEV BBs to be fully enclosed for lower computation complexity.

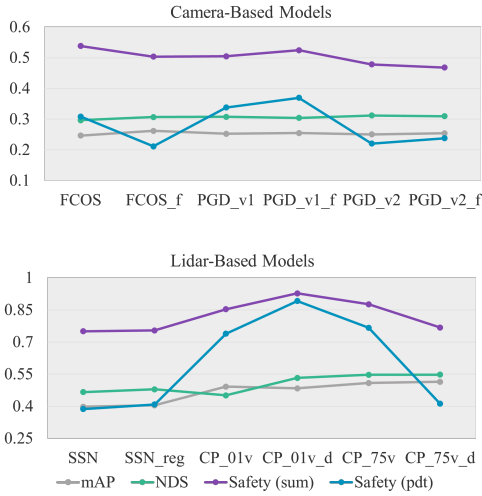


Fig. 6: Evaluation results of different object detectors (trained and provided by [2]) using mean Average Precision (mAP), nuScenes Detection Score (NDS), and our safety metrics formed by averaging (sum) and multiplication (pdt).

saturates when the prediction reaches a “safe” state. Hence, we combine the safety loss component with the state-of-the-art loss functions for accurate object detection (L_{Acc}), e.g., the SmoothL1 Loss ($L_{SmoothL1}$) [23] or the Efficient-IoU Loss (L_{EffIoU}) [9]. Altogether, we have:

$$L_{Safe-Acc}(\mathbf{B}_{3D}^{PD}, \mathbf{B}_{3D}^{GT}) = \lambda L_{IoGT}(\mathbf{B}_{3D}^{PD}, \mathbf{B}_{3D}^{GT}) + (1 - \lambda) L_{Acc}(\mathbf{B}_{3D}^{PD}, \mathbf{B}_{3D}^{GT}), \quad (8)$$

where $\lambda \in \mathbb{R} : 0 < \lambda \leq 1$ is a balancing hyper-parameter. In practice, this hyper-parameter can be tuned during a learning process (similar to the NN learning rate) to favor accuracy at early episodes and improve safety in the end. Finally, we note that L_{Acc} can be instantiated by different loss functions depending on the need of the NN architectures, giving another degree of flexibility.

VII. EXPERIMENTAL RESULTS AND DISCUSSIONS

We now provide and discuss the experimental settings and results. For experiment, we utilize the public 3D object detection library MMDetection3D [2] and run models on the nuScenes dataset [24] and an in-house simulation dataset⁹.

A. Evaluating Object Detectors with the Safety Metric

We perform the model evaluation step in a general NN learning pipeline to see our safety metrics’ effectiveness. We select the leading models on the nuScenes dataset, including the camera-based FCOS3D [25] and PGD [26] as well as the lidar-based CenterPoint [27] and SSN [28]. We also consider their variants generated with different backbones, voxel sizes, or finetuning steps. The relevant details can be found in [2]. We record the evaluation results in Fig. 6 and highlight the following three observations: First, as typically perceived, the lidar-based models are more reliable than camera-based

ones, and our safety metrics confirm this. Second, our safety metrics are by themselves consistent and depict different performance profiles from the accuracy metrics (i.e., mean Average Precision (mAP) and nuScenes Detection Score (NDS) [24]). In particular, our multiplication-based metric (i.e., Safety (pdt)) can significantly differentiate the model performance better than the other metrics with the identification of much more unsafe cases. Finally, we see that more accurate models are not necessarily safer, according to our definition in Requirement (1).

B. Optimizing Object Detectors with Safety Losses

We now close the loop of our work by conducting optimization with an instantiation of the safety-aware loss function. We utilize the state-of-the-art monocular 3D object detector FCOS3D [25] and follow the original paper to implement the SmoothL1 loss. We also apply the optimization settings, such as data augmentation, batch sizes, and learning schemes, as reported in [2].

1) *Training on the nuScenes Dataset:* Here, we utilize the nuScenes-mini dataset [24] and conduct full training from scratch for 20 epochs. As mentioned, we make a baseline model, which we call FCOS.a, by training FCOS3D with the SmoothL1 loss [25]. For safety improvement, we keep the SmoothL1 loss as the accuracy loss component (i.e., $L_{Acc} = L_{SmoothL1}$) and set λ in the safety loss function (8) to 0.2 to train the model, which we call FCOS.s.

As seen in Fig. 7a, qualitatively, the highlighted surrounding vehicles are better detected by FCOS.s. This is likely attributed to the explicit optimization of the safety loss component (i.e., the IoGT measure). Then, for a quantitative evaluation, we evaluate both models with mAP and our multiplicative safety metric (i.e., (7)). From Fig. 7b, we observe that despite slightly more fluctuating and slower, FCOS.s still achieves similar accuracy to FCOS.a in later epochs. More importantly, it contributes to more stable and much higher safety scores.

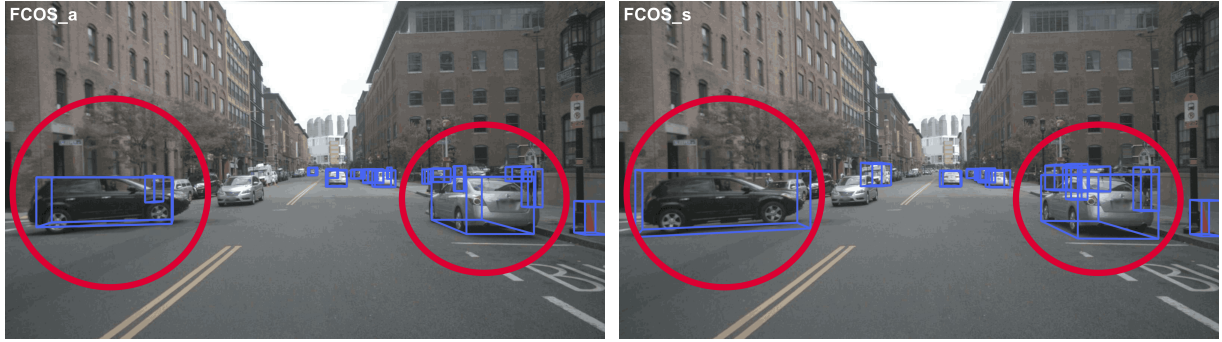
2) *Finetuning on a Simulation Dataset:* We further perform experiments with our in-house simulation dataset. Under the scope of the EU-funded FOCETA project¹⁰, we utilize the Simcenter Prescan simulator¹¹ to collect a set of data to train and test object detectors. More specifically, this FOCETA dataset focuses on parking scenarios with walking pedestrians and clustered vehicles. We apply the same settings from above, including the baseline object detector, FCOS, and the loss functions. The only difference is that we perform finetuning for 10 epochs here (instead of training from scratch).

Qualitatively, in Fig. 8a, the FCOS.s model again produces a better BB to contain the entirety of the pedestrians; quantitatively, a similar trend is observed in Fig. 8b: The model finetuned with the safety-aware loss function delivers a similar number of accurate predictions yet reduced many

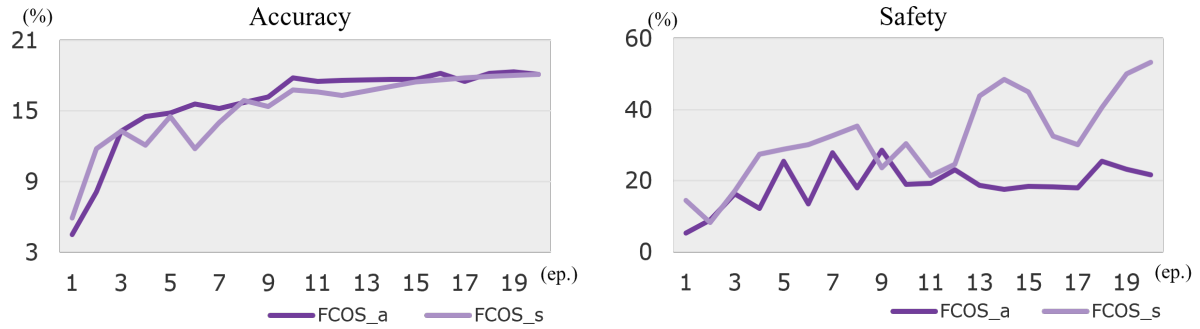
⁹The utilization of the MMDetection3D library and nuScenes dataset in this paper is for knowledge dissemination and scientific publication, not for commercial use.

¹⁰<http://www.foceta-project.eu/>

¹¹<https://plm.sw.siemens.com/de-DE/simcenter/autonomous-vehicle-solutions/prescan/>

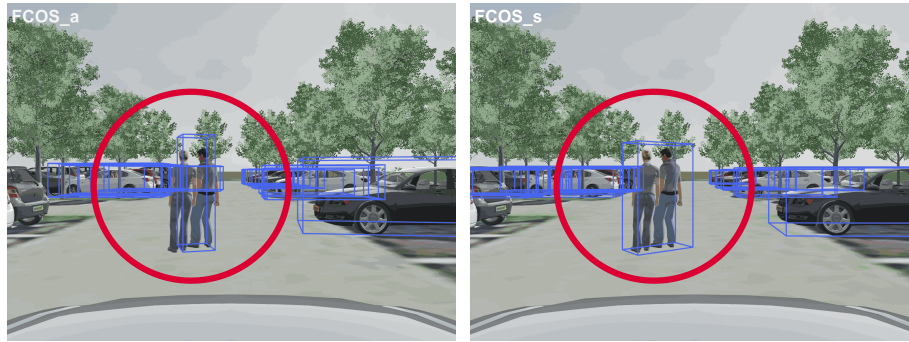


(a) Qualitative results.

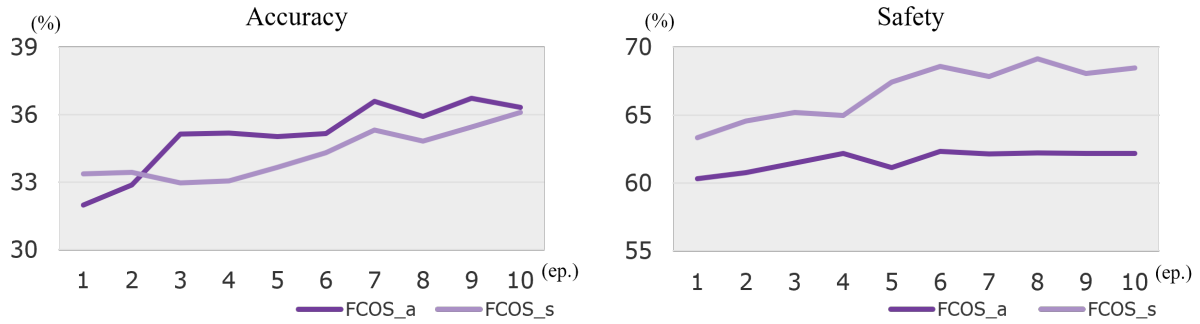


(b) Quantitative evaluation.

Fig. 7: Training results on the nuScenes-mini dataset.



(a) Qualitative results.



(b) Quantitative evaluation.

Fig. 8: Finetuning results on the FOCETA dataset.

unsafe cases. One small difference here is that the performance curves are smoother than those in Fig. 7b, possibly thanks to the fact that the models are pre-trained before finetuning.

VIII. CONCLUSION

This work considers evaluating and improving object detectors in AD with respect to safety. We define safety in AD contexts as the object detector always predicting objects not farther than their ground truth with full coverage. This helps reduce the risk of colliding with objects at their fronts. We formalize the requirement by abstracting real-world 3D objects with 2D PV BBs and BEV BBs and derive a safety metric for the actual evaluation of object detectors (regardless of the underlying sensing technology, e.g., camera, lidar or radar). In addition, we propose a safety-aware loss function for model optimization. Our proposals are shown to be practical and valid with the experiments: The safety metric depicts different performance profiles from those given by accuracy metrics such as mAP, and our loss function reduces unsafe predictions while maintaining accuracy and stability during optimizing sessions.

Still, there are certain limitations in this work, and they open interesting directions. First, we consider only single-step input-output relations, whereas real-world systems involve time and motion. One natural extension is to investigate safety requirements for object tracking and trajectory prediction components. Likewise, future studies can identify more safety properties of object detectors. Second, larger-scale experiments are required to see the generalizability of our proposals to more models. Third, the safety-aware loss function can be improved, for instance, by using importance weighting schemes or merging the safety and accuracy loss components through a mechanism beyond a simple coefficient. Lastly, from the perspective of AVs, our work considers only a component-level requirement. Whether this requirement benefits system-level safety is still to be investigated.

REFERENCES

- [1] X. Ma, W. Ouyang, A. Simonelli, and E. Ricci, “3D object detection from images for autonomous driving: A survey,” *arXiv preprint arXiv:2202.02980*, 2022.
- [2] M. Contributors, “MMDetection3D: OpenMMLab next-generation platform for general 3D object detection,” <https://github.com/open-mmlab/mmdetection3d>, 2020.
- [3] R. Padilla, S. L. Netto, and E. A. B. da Silva, “A survey on performance metrics for object-detection algorithms,” 2020.
- [4] R. Padilla, W. L. Passos, T. L. B. Dias, S. L. Netto, and E. A. B. da Silva, “A comparative analysis of object detection metrics with a companion open-source toolkit,” *Electronics*, 2021.
- [5] T.-Y. Lin, P. Goyal, R. Girshick, K. He, and P. Dollar, “Focal loss for dense object detection,” in *ICCV*, 2017.
- [6] J. Yu, Y. Jiang, Z. Wang, Z. Cao, and T. Huang, “Unitbox: An advanced object detection network,” in *ACM Multimedia*, 2016.
- [7] H. Rezatofighi, N. Tsoi, J. Gwak, A. Sadeghian, I. Reid, and S. Savarese, “Generalized IoU,” in *CVPR*, 2019.
- [8] Z. Zheng, P. Wang, W. Liu, J. Li, R. Ye, and D. Ren, “Distance-IoU loss: Faster and better learning for bounding box regression,” in *AAAI*, 2020.
- [9] Y.-F. Zhang, W. Ren, Z. Zhang, Z. Jia, L. Wang, and T. Tan, “Focal and efficient IoU loss for accurate bounding box regression,” *Neurocomputing*, vol. 506, pp. 146–157, 2022.
- [10] S. Houben, S. Abrecht, M. Akila, A. Bär, F. Brockherde, P. Feifel, T. Fingscheidt, S. S. Gannamaneni, S. E. Ghobadi, A. Hammam, A. Haselhoff, F. Hauser, C. Heinzemann, M. Hoffmann, N. Kapoor, F. Kappel, M. Klingner, J. Kronenberger, F. Küppers, J. Löhdefink, M. Mlynarski, M. Mock, F. Mualla, S. Pavlitskaya, M. Poretschkin, A. Pohl, V. Ravi-Kumar, J. Rosenzweig, M. Rottmann, S. Rüping, T. Sämann, J. D. Schneider, E. Schulz, G. Schwalbe, J. Sicking, T. Srivastava, S. Varghese, M. Weber, S. Wirkert, T. Wirtz, and M. Woehrle, “Inspect, understand, overcome: A survey of practical methods for AI safety,” in *Deep Neural Networks and Data for Automated Driving*. Springer International Publishing, 2022, pp. 3–78.
- [11] J. Guo, U. Kurup, and M. Shah, “Is it safe to drive? An overview of factors, metrics, and datasets for driveability assessment in autonomous driving,” *IEEE Trans. Intell. Transp. Syst.*, 2020.
- [12] M. Kwiatkowska, G. Norman, and D. Parker, “Prism: Probabilistic model checking for performance and reliability analysis,” *SIGMETRICS Perform. Eval. Rev.*, vol. 36, p. 40–45, 2009.
- [13] X. Huang, D. Kroening, W. Ruan, J. Sharp, Y. Sun, E. Thamo, M. Wu, and X. Yi, “A survey of safety and trustworthiness of deep neural networks: Verification, testing, adversarial attack and defence, and interpretability,” *Computer Science Review*, vol. 37, p. 100270, 2020.
- [14] C.-H. Cheng, A. Knoll, and H.-C. Liao, “Safety metrics for semantic segmentation in autonomous driving,” in *AITest*, 2021.
- [15] S. Shalev-Shwartz, S. Shammah, and A. Shashua, “On a formal model of safe and scalable self-driving cars,” 2017.
- [16] G. Volk, J. Gamerdinger, A. v. Bernuth, and O. Bringmann, “A comprehensive safety metric to evaluate perception in autonomous systems,” in *ITSC*, 2020.
- [17] C.-H. Cheng, T. Schuster, and S. Burton, “Logically sound arguments for the effectiveness of ml safety measures,” in *SafeComp Workshops*, 2022.
- [18] F. de Grancey, J.-L. Adam, L. Alecu, S. Gerchinovitz, F. Mamalet, and D. Vigouroux, “Object detection with probabilistic guarantees: A conformal prediction approach,” in *SafeComp Workshops*, 2022.
- [19] T. Schuster, E. Seferis, S. Burton, and C.-H. Cheng, “Unaligned but safe – formally compensating performance limitations for imprecise 2d object detection,” in *SafeComp*, 2022.
- [20] H. Kaulbersch, J. Honer, and M. Baum, “A cartesian b-spline vehicle model for extended object tracking,” in *FUSION*, 2018.
- [21] B. Chen, C. Gong, and J. Yang, “Importance-aware semantic segmentation for autonomous vehicles,” *IEEE Transactions on Intelligent Transportation Systems*, 2019.
- [22] N. Ravi, J. Reizenstein, D. Novotny, T. Gordon, W.-Y. Lo, J. Johnson, and G. Gkioxari, “Accelerating 3D deep learning with pytorch3d,” 2020.
- [23] R. Girshick, “Fast R-CNN,” in *ICCV*, 2015.
- [24] H. Caesar, V. Bankiti, A. H. Lang, S. Vora, V. E. Liong, Q. Xu, A. Krishnan, Y. Pan, G. Baldan, and O. Beijbom, “nuScenes: A multimodal dataset for autonomous driving,” *arXiv preprint arXiv:1903.11027*, 2019.
- [25] T. Wang, X. Zhu, J. Pang, and D. Lin, “FCOS3D: Fully convolutional one-stage monocular 3D object detection,” in *ICCVW*, 2021.
- [26] —, “Probabilistic and Geometric Depth: Detecting objects in perspective,” in *CoRL*, 2021.
- [27] T. Yin, X. Zhou, and P. Krähnenbühl, “Center-based 3D object detection and tracking,” in *CVPR*, 2021.
- [28] X. Zhu, Y. Ma, T. Wang, Y. Xu, J. Shi, and D. Lin, “SSN: Shape signature networks for multi-class object detection from point clouds,” in *ECCV*, 2020.